Rapid Communications

Natural abundance ^{17}O and ^{33}S nuclear magnetic resonance spectroscopy in solids achieved through extended coherence lifetimes

Daniel Jardón-Álvarez,[1] Mark O. Bovee,[1] Jay H. Baltisberger,[2] and Philip J. Grandinetti[1,*]

[1]*Department of Chemistry, Ohio State University, 100 West 18th Avenue, Columbus, Ohio 43210, USA*

[2]*Division of Natural Science, Mathematics, and Nursing, Berea College, Berea, Kentucky 40403, USA*

(Received 10 August 2019; published 28 October 2019)

We have found that the NMR coherence lifetime T_2 of the symmetric central ($\pm\frac{1}{2} \rightarrow \mp\frac{1}{2}$) transition for ^{17}O nuclei through a π pulse train can be extended by over two orders of magnitude in a lattice dilute with NMR active nuclei through the use of highly selective (low-power) radio-frequency pulses. Crucial to this lifetime extension is the avoidance of coherence transfer to short-lived nonsymmetric transitions. For ^{17}O in α-quartz, we obtain $T_2 = 262 \pm 1$ s. This translates into enormous sensitivity gains for echo train acquisition schemes such as Carr-Purcell-Meiboom-Gill (CPMG). By combining satellite population transfer schemes with a low-power (2.73 kHz) CPMG on ^{17}O in quartz, we obtain over a 1000-fold sensitivity enhancement compared to a spectrum from a free induction decay acquired at a more typical rf field strength of 32.5 kHz. For ^{33}S in K_2SO_4 the same approach yields $T_2 = 8.8 \pm 0.4$ s and a sensitivity enhancement of 63. In both examples, these enhancements enable the acquisition of NMR spectra at 9.4 T, despite their low natural abundance and spin-lattice relaxation times of ~900 and 25 s, respectively, with signal-to-noise ratios of ~30 in 1 h.

DOI: 10.1103/PhysRevB.100.140103

In a multipulse nuclear magnetic resonance (NMR) experiment, an ensemble of nuclear spins is coherently evolved while being transferred through a pathway of spin transitions [1]. A critical factor in the success of most multipulse NMR experiments is that the overall coherence lifetime through this spin transition pathway is longer than the pulse sequence. The overall decoherence through a given transition pathway is a time-weighted average of the decoherence rates, $1/T_2^{m-m'}$, associated with each transition $m \rightarrow m'$ in the pathway. In a quadrupolar nucleus, it is well known [2–6] that transitions experiencing the first-order quadrupolar interaction, e.g., the satellite transitions, experience shorter T_2 values than the symmetric transitions, i.e., $m \rightarrow -m$. This is a consequence of transverse relaxation of the symmetric transitions being unaffected by secular contributions which are proportional to the spectral density function at zero frequency [3,7]. Therefore, in the design and implementation of any multipulse NMR experiments, the overall coherence lifetime through the measured transition pathways can be extended if these "killing" transitions, where strong decoherence occurs, are avoided.

We have discovered a remarkable illustration of this effect in half-integer quadrupolar nuclei where the overall coherence lifetime in a Carr-Purcell-Meiboom-Gill (CPMG) echo train [8–10] can be significantly extended by avoiding coherence transfer to any transition experiencing a strong first-order (secular) quadrupolar interaction. This is illustrated in Fig. 1, comparing the echo train coherence lifetime of two ^{17}O signals during magic-angle spinning (MAS) in a polycrystalline sample of ^{17}O-enriched (40 %) coesite [12], a silica polymorph, using rf field strengths of $\omega_1/(2\pi) = 72.5$ kHz and 182 Hz, respectively. The lower rf field strength makes the π pulses more selective to the symmetric central ($m = \pm\frac{1}{2} \rightarrow \mp\frac{1}{2}$) transition, reduces undesired excitations of the satellite and other transitions experiencing

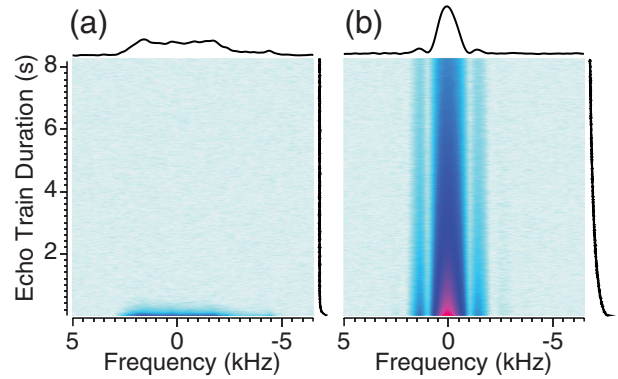

FIG. 1. The ^{17}O MAS CPMG nuclear spin echo train decay in ^{17}O-enriched polycrystalline coesite (SiO_2) at 9.4 T comparing rf field strengths of (a) $\omega_1/(2\pi) = 72.5$ kHz and (b) 182 Hz. The echo train dimension is on the vertical axis and the frequency dimension is on the horizontal axis. The echo trains follow a stretched exponential decay [11] in (a) with T_2 of 70 ± 5 ms and a Kohlrausch exponent of $\beta = 0.72 \pm 0.03$, and in (b) with T_2 of 2.55 ± 0.01 s and $\beta = 0.542 \pm 0.002$. A T_1 of ~400 s was determined and a recovery delay of 600 s was used. In both measurements 1024 π pulses were applied with a spacing of $\tau_1 = 8$ ms and 64 scans were averaged. The one-dimensional (1D) signals above and to the right of each spectrum are the horizontal and vertical cross sections taken at the highest intensity.

*www.grandinetti.org

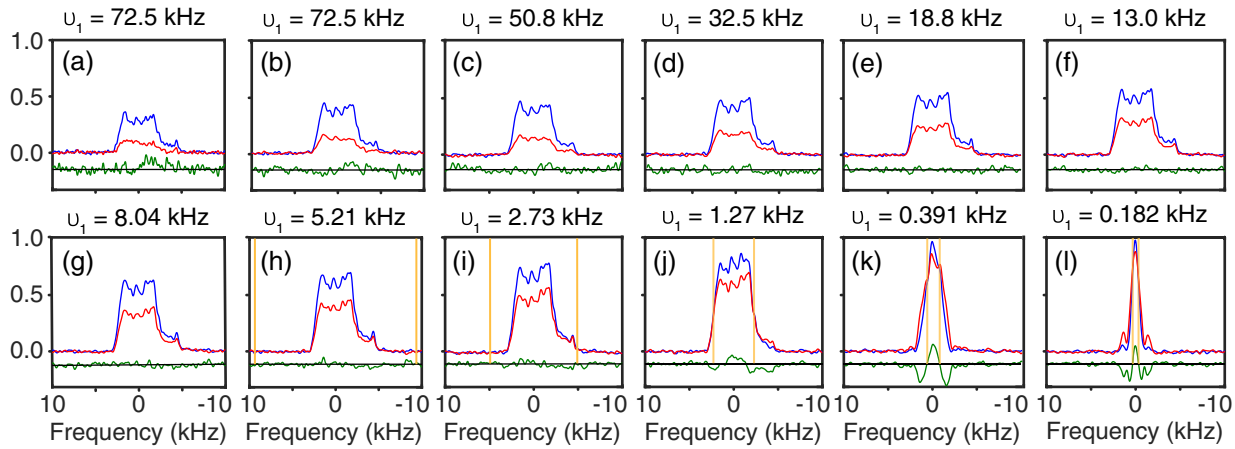

FIG. 2. Comparison of the ^{17}O MAS NMR spectra of polycrystalline coesite at 9.4 T from the first and 15th echoes obtained with CPMG using square pulses for different rf field strengths as indicated above each spectrum. Echo 1 is depicted in blue, echo 15 is depicted in red, the residual difference between the two after renormalizing intensities is depicted in green, and the sinc excitation profile full width at half maximum (FWHM) is depicted in orange. For powers above $\omega_1/(2\pi) = 5.21$ kHz, the excitation profile FWHM is wider than the plot's window. In (a) the $\pi/2$ and π pulse lengths of 1.8 and 3.4 μs, respectively, were determined from the first maximum and null of a nutation measurement on the coesite ^{17}O signal. In (b)–(l) the $\pi/2$ and π pulse lengths were then set to the theoretical values of $\pi/(6\omega_1)$ and $\pi/(3\omega_1)$, respectively, for the central transition of the $I = 5/2$ nucleus. All π pulses had a spacing of 8 ms. Further experimental details are given in the Supplemental Material [13].

the stronger first-order quadrupolar interaction, and, in this comparison, extends the coherence lifetime by a factor of 30.

This behavior is systematically examined in Fig. 2 using the ^{17}O anisotropic central transition MAS line shapes in coesite [12]. In Fig. 2(a) [and also in Fig. 1(a)], the $\pi/2$ and π pulse lengths were determined from the first maximum and null of a nutation measurement on the coesite ^{17}O signal. In Figs. 2(b)–2(l) [and also in Fig. 1(b)], the $\pi/2$ and π pulse lengths were set to the theoretical values [14] of $\pi/(6\omega_1)$ and $\pi/(3\omega_1)$, respectively, for the central transition of the $I = 5/2$ nucleus based on rf field strengths calibrated using the natural abundance ^{17}O resonance in liquid water. In Fig. 2 the higher-intensity central transition spectrum is from the first echo (blue) and the lower-intensity spectrum is from the 15th echo (red). First of all, we note the slight sensitivity improvement by setting the $\pi/2$ and π pulse lengths to the theoretical values instead of the values determined by a nutation measurement on coesite. More significantly, however, we find that the amplitudes of both the first and 15th echoes increase from Fig. 2(b) to Fig. 2(l) with decreasing rf power.

Additionally, one can see in Fig. 2 that the difference in the first and 15th echo amplitudes decreases with decreasing rf power, a reflection of the increasing overall coherence lifetime through the transition pathway leading to the 15th echo. The echo train coherence lifetime continues to increase even as the π pulse bandwidth is less than the anisotropic central transition linewidth, as seen in Figs. 2(k) and 2(l). This is because the low-intensity anisotropic center band line shape of the inner satellite transitions (indiscernible here) is partially overlapping with the high-frequency side of the central transition center band line shape. Thus, it is only when the excitation pulse bandwidth is inside the central transition line shape that the pulse can become truly central transition selective.

The difference between the first and 15th echo amplitudes, after renormalizing by minimizing the sum of the residuals, is shown in green below the spectra for each rf field strength in Fig. 2. Inspection of these residuals reveals no significant anisotropy in the echo train decoherence at the rf powers where excitation of the anisotropic line shape is not bandwidth limited. Improved central transition selectivity without loss of integrity of its anisotropic line shape can be obtained by using Gaussian-shaped π pulses instead of square pulses.

The ultimate limit to the echo train coherence lifetime is the intrinsic T_2 of the central transition. In this polycrystalline silica sample isotopically enriched to 40 % ^{17}O, however, the echo train coherence lifetime is limited by homonuclear dipolar couplings between ^{17}O nuclei which create a homogenous interaction that broadens all ^{17}O transitions and cannot be completely refocused by MAS and the π pulse train. At ^{17}O natural abundance levels of 0.037 %, the limiting factor for this coherence lifetime in a similar SiO_2 material will be a heteronuclear coupling to the 4.7 % abundant ^{29}Si nuclei. Specifically, the many-body homonuclear couplings among the ^{29}Si nuclei make this interaction homogenous and not fully refocused by MAS and the π pulse train [15]. At ^{17}O natural abundance levels, this latter homogeneous interaction is typically orders of magnitude smaller than the former in the ^{17}O-enriched samples. Thus, we can expect even greater echo train coherence lifetime enhancements in a SiO_2 material with decreasing rf power at ^{17}O natural abundance. This is nicely illustrated in Fig. 3 with the ^{17}O natural abundance echo train decays of polycrystalline quartz, comparing the use of square π pulses at an rf field strength of 32.5 kHz to Gaussian-shaped π pulses with a maximum rf field strength of 2.73 kHz. In this sample, where the spin-lattice relaxation time is $T_1 \approx 900$ s, the reduction in rf power increases the echo train coherence lifetime from $T_2 = 1.02 \pm 0.08$ s to $T_2 = 262 \pm 1$ s, i.e., by

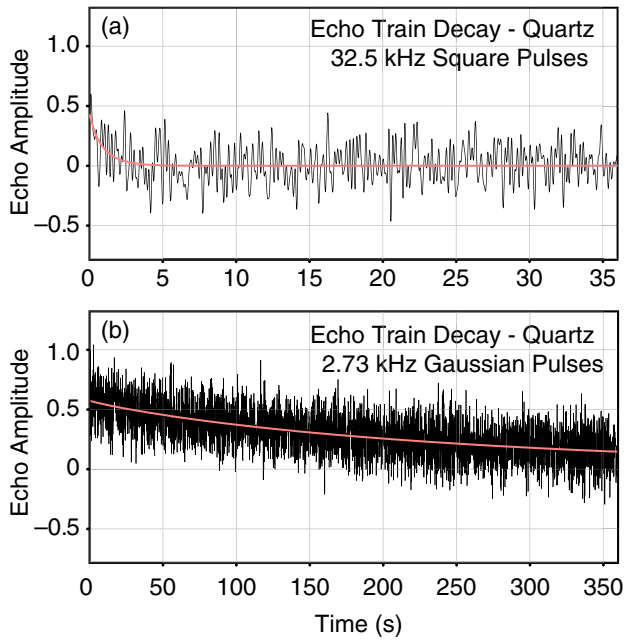

FIG. 3. ^{17}O CPMG decay of polycrystalline quartz using high-power square and low-power Gaussian pulses. The measured decays are depicted in black while the best-fit stretched exponential decays are depicted in red. The echo train acquisition employed a train of 60 000 π pulses with a 6 ms spacing. An rf field strength of $\omega_1/(2\pi) = 32.5$ kHz was used for the square π pulse train while $\omega_1/(2\pi) = 2.73$ kHz was used for the Gaussian π pulse train. Both decays (24 scan average) were filtered in the inverse (frequency) domain with a top-hat filter using cutoffs of ± 5 Hz. The best fit to exponential decays give $T_2 = 1.02 \pm 0.08$ s for the higher-power square π pulse train decay, and $T_2 = 262 \pm 1$ s for the lower-power Gaussian π pulse train decay. This represents a 260-fold increase in the echo train coherence lifetime. The sensitivity enhancement associated with lowering the rf field strength, determined from the ratio of the initial amplitudes obtained in the fits, is $\eta^{\text{lp}} = 1.44$.

a factor of 260. It should be remarked that this T_2 increase could be made more dramatic by comparing to higher rf powers where the echo train coherence lifetimes are shorter. The correlated loss of intensity at higher rf powers, however, makes such measurements impractically long. That said, the conventional wisdom [16,17] for selective excitation of the central transition, $\omega_q/\omega_1 > 4.5$, leads to rf field strengths on the order of the higher value used in Fig. 3(a) for the ^{17}O central transition [18,19], with the corresponding and significantly shorter echo train coherence lifetimes. Thus, we conclude that it is always beneficial, and without any disadvantage, to go to the lowest possible rf powers within the constraints of the required excitation bandwidth.

As echo train acquisition is a common approach for enhancing sensitivity in solid-state NMR [20], such an increase in coherence lifetime can translate into enormous sensitivity gains. For a given π pulse spacing τ_1, one expects a CPMG sensitivity enhancement on the order of $\eta^{\text{ETA}} \propto \sqrt{T_2/\tau_1}$. In the coesite study in Fig. 2, we find that the largest echo train sensitivity enhancement with minimal line-shape distortion is obtained using an rf field strength around 2.73 kHz. In this case, we obtain $\eta^{\text{ETA}} = 8.6$ compared to a free induction decay at the same rf power. If experimental quantification of η^{ETA} cannot be obtained because the free induction decay sensitivity is too low for observation, then η^{ETA} can be numerically estimated from a fit of the exponential decay. Additionally, we define η^{lp}, the sensitivity enhancement associated with lowering the rf power, as the amplitude ratio of the first echoes at the two rf powers. For coesite, we obtain $\eta^{\text{lp}} = 1.6$ by reducing the rf field strength from 32.5 to 2.73 kHz. The initial magnetization associated with the central transition can be further enhanced by using rotor assisted population transfer (RAPT) to saturate the satellite transition magnetization [21–23]. Combining the aforementioned enhancements with that of RAPT, $\eta^{\text{RAPT}} = 2.5$, we obtain a total sensitivity enhancement of 34.4 relative to a free induction decay acquired at 32.5 kHz.

A more impressive example of the impact of this extended coherence lifetime is shown in Fig. 4(a). Here is an ^{17}O natural abundance spectrum of crystalline α-quartz acquired with two scans of "soft" CPMG (116 000 echoes/scan) in 48 min giving a signal-to-noise ratio of 32. At an rf field strength of 2.75 kHz, the echo train enhancement alone is $\eta^{\text{ETA}} = 281$ compared to a free induction decay at this rf power. In this example, the soft CPMG is also prefaced with RAPT, which by itself gives a sensitivity enhancement of about $\eta^{\text{RAPT}} = 2.5$. Taken together with the enhancement of reduced power, $\eta^{\text{lp}} = 1.44$, we obtain a total sensitivity enhancement that is slightly over 1000 relative to a free induction decay acquired at 32.5 kHz, which of course translates into *a millionfold decrease in the signal averaging time.* Analysis of the α-quartz ^{17}O line shape, taking echo truncation into account [24], gives quadrupolar coupling parameters of $C_q = 5.15$ MHz, $\eta_q = 0.21$, and $\delta_{\text{iso}} = 41.7$ ppm, consistent with previously measured values by Larsen and Farnan [18] on ^{17}O-enriched quartz. Note that the ^{17}O coherence lifetime in α-quartz decreases from 262 to 170 s in the measurements of Figs. 3(b) and 4(a) as the number of π pulses is increased from 60 000 to 116 000, and the π pulse spacing is decreased from 6 to 2 ms, respectively. This is likely the result of cumulative loss from rf field inhomogeneities or added excitation of short-lived nonsymmetric transitions, or both. This suggests that further sensitivity gains may be had by improving the rf field homogeneity of the transmitter coil and employing shaped pulses with better bandwidth selectivity.

Among the $I = 3/2$ nuclides in the periodic table ^{33}S is an example of a low natural abundance (0.75 %) nuclide of broad interest. Its NMR sensitivity is further limited by a low gyromagnetic ratio. An example of a natural abundance ^{33}S NMR sensitivity enhancement using soft CPMG is shown in Fig. 4(b) for K_2SO_4. In K_2SO_4 there is a single ^{33}S site with a C_q of ~1 MHz. At an rf field strength of 2.76 kHz, we obtain an echo train coherence lifetime of $T_2 = 8.8 \pm 0.4$ s, which leads to $\eta^{\text{ETA}} = 36$. Taken together with a RAPT enhancement of $\eta^{\text{RAPT}} = 1.75$, we obtain an overall sensitivity enhancement of 63 relative to a free induction decay at the *same* rf power. While this sensitivity is substantial, it is not as large as what was obtained for ^{17}O in quartz. This is primarily due to the upper limit on T_2 placed by the shorter spin-lattice relaxation time of $T_1 = 25$ s. Additionally, the narrower anisotropic line shape requires longer echo spacings

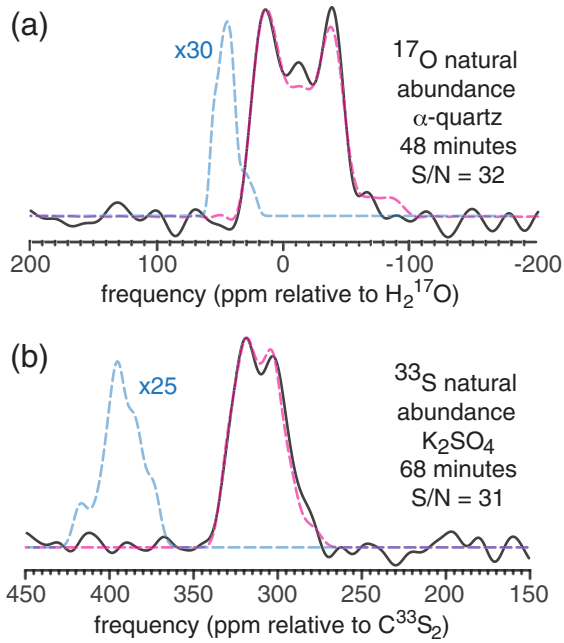

FIG. 4. Natural abundance MAS NMR spectra of (a) ^{17}O in α-quartz and (b) ^{33}S in K_2SO_4 obtained using RAPT-soft-CPMG echo train acquisition at a MAS spinning rate of $\nu_R = 14$ kHz. In (a), the soft-CPMG train of Gaussian-shaped π pulses with a maximum rf field strength of $\omega_1/(2\pi) = 2.73$ kHz and a spacing of 2 ms was used to acquire 116 000 echoes. Two scans were performed for a total of 48 min. In (b), the CPMG sequence, consisting of a train of square π pulses with an rf field strength of $\omega_1/(2\pi) = 2.76$ kHz and a spacing of 6 ms, was used to acquire 2000 echoes. With 128 scans, this measurement required 68 min. Fits of the echo decays give (a) $T_2 = 170 \pm 20$ s and (b) $T_2 = 8.8 \pm 0.4$ s. The echo train acquisition signal was processed as described by Dey *et al.* [24] to obtain the 1D spectra shown above. This combination of RAPT and soft CPMG yields a sensitivity enhancement in (a) of over a 1000-fold relative to a free induction decay acquired at 32.5 kHz, and in (b) of 64 relative to a free induction decay acquired at the same rf field strength. Further experimental details for both measurements are given in the Supplemental Material [13]. The dashed red line represents the best-fit central transition line shape while the dashed blue line represents the corresponding inner satellite transition center band line shape with the amplitude scaling factor shown alongside.

for resolving spectral features, which also leads to a reduction in the echo train enhancement.

The frequency offset between the central and satellite transition MAS center bands and the low relative amplitudes of the satellite transition center and sidebands are what make selective central transition excitation possible. This is illustrated in Fig. 4 with simulated satellite transition center bands (scaled up) shown in blue dashed lines. For $I = 3/2$ nuclei, there is a fixed gap between the highest-frequency singularity (edge) of the central transition center band and the lowest-frequency singularity (edge) of the satellite transition center band line shape, given by [1,25]

$$\Delta\omega_{\text{gap}} = \left(\omega_q^2/\omega_0\right)(135 - 102\eta + 79\eta^2)/756, \qquad (1)$$

making it somewhat easier to obtain selective central transition excitation of $I = 3/2$ nuclei. This center band gap is $\Delta\omega_{\text{gap}} \sim 1$ kHz for ^{33}S in K_2SO_4. For $I > 3/2$ half-integer nuclei, however, the anisotropic center band of the innermost satellite transition is always partially overlapping with the central transition. Selective central transition excitation, however, is still aided by the considerably lower amplitude of the satellite transition center and sidebands at low MAS speeds [26,27].

Examples of long-lived echo train lifetimes are known in a lattice depleted of NMR active nuclei [28,29] or under cryogenic temperatures [30]. Here, we have shown that similar long-lived coherences are possible for the central transition of half-integer quadrupolar nuclei in a lattice of NMR inactive nuclei if the excitation can be made truly selective on the central transition, i.e., avoiding any excitation and coherence loss to short-lived nonsymmetric transitions. To our knowledge, the T_2 of 262 s in ^{17}O in quartz is the longest nuclear spin coherence lifetime measured under ambient conditions. Clearly, the impact of this effect on NMR sensitivity enhancements through echo train acquisition is profound. Beyond the sensitivity enhancement for NMR structural studies, this understanding for extending coherence lifetimes could translate into improved quantum information devices [31]. The needs for a high T_2/T_1 ratio for the central transition and a lattice dilute in NMR active nuclei present a clear limitation for this approach. It would, for example, be less successful for natural abundance ^{17}O in organic solids due to the strong decoherence from heteronuclear dipolar couplings to the bath of coupled protons. In this sense, the soft-CPMG approach to sensitivity enhancement is complementary to approaches where enhanced polarization is transferred from hyperpolarized magnetic centers via spin diffusion of abundant NMR active nuclei [32,33].

The authors thank Prof. Jonathan Stebbins for the loan of the ^{17}O-enriched coesite sample. This material is based upon work supported in part by the National Science Foundation under Grant No. CHE-1807922.

[1] P. J. Grandinetti, J. T. Ash, and N. M. Trease, Prog. Nucl. Magn. Reson. Spectrosc. **59**, 121 (2011).
[2] P. S. Hubbard, J. Chem. Phys. **53**, 985 (1970).
[3] D. Petit and J.-P. Korb, Phys. Rev. B **37**, 5761 (1988).
[4] T. Vosegaard, J. Skibsted, H. Bildsoe, and H. J. Jakobsen, J. Magn. Reson. **122**, 111 (1996).
[5] S. E. Ashbrook, S. Antonijevic, A. J. Berry, and S. Wimperis, Chem. Phys. Lett. **364**, 634 (2002).
[6] M. J. Thrippleton, M. Cutajar, and S. Wimperis, Chem. Phys. Lett. **452**, 233 (2008).
[7] G. Wu, Prog. Nucl. Magn. Reson. Spectrosc. **114-115**, 135 (2019).
[8] H. Y. Carr and E. M. Purcell, Phys. Rev. **94**, 630 (1954).
[9] S. Meiboom and D. Gill, Rev. Sci. Instrum. **29**, 688 (1958).
[10] C. P. Slichter, *Principles of Magnetic Resonance* (Springer, Berlin, 1980).

[11] F. Devreux, J. P. Boilot, F. Chaput, and B. Sapoval, Phys. Rev. Lett. **65**, 614 (1990).
[12] P. J. Grandinetti, J. H. Baltisberger, U. Werner, A. Pines, I. Farnan, and J. F. Stebbins, J. Phys. Chem. **99**, 12341 (1995).
[13] See Supplemental Material at http://link.aps.org/supplemental/10.1103/PhysRevB.100.140103 for additional experimental details on the NMR pulse sequence, acquisition parameters, and data analysis.
[14] A. Abragam, *Principles of Nuclear Magnetism* (Oxford University Press, Oxford, UK, 1961).
[15] M. M. Maricq and J. S. Waugh, J. Chem. Phys. **70**, 3300 (1979).
[16] F. H. Larsen, H. J. Jacobsen, P. D. Ellis, and N. C. Nielsen, J. Phys. Chem. A **101**, 8597 (1997).
[17] F. H. Larsen, H. J. Jakobsen, P. D. Ellis, and N. C. Nielsen, J. Magn. Reson. **131**, 144 (1998).
[18] F. H. Larsen and I. Farnan, Chem. Phys. Lett. **357**, 403 (2002).
[19] S. E. Ashbrook and I. Farnan, Solid State NMR **26**, 105 (2004).
[20] N. M. Szeverenyi, A. Bax, and G. E. Maciel, J. Magn. Reson. **61**, 440 (1985).
[21] Z. Yao, H.-T. Kwak, D. Sakellariou, L. Emsley, and P. J. Grandinetti, Chem. Phys. Lett. **327**, 85 (2000).
[22] S. Prasad, H. T. Kwak, T. Clark, and P. J. Grandinetti, J. Am. Chem. Soc. **124**, 4964 (2002).
[23] N. M. Trease, K. K. Dey, and P. J. Grandinetti, J. Magn. Reson. **200**, 334 (2009).
[24] K. Dey, J. T. Ash, N. M. Trease, and P. J. Grandinetti, J. Chem. Phys. **133**, 054501 (2010).
[25] D. Müller, Ann. Phys. **494**, 451 (1982).
[26] P. Caravatti, G. Bodenhausen, and R. R. Ernst, J. Magn. Reson. **55**, 88 (1983).
[27] A. Pell, G. Kervern, L. Emsley, M. Deschamps, D. Massiot, P. J. Grandinetti, and G. Pintacuda, J. Chem. Phys. **134**, 024117 (2011).
[28] T. D. Ladd, D. Maryenko, Y. Yamamoto, E. Abe, and K. M. Itoh, Phys. Rev. B **71**, 014401 (2005).
[29] K. Saeedi, S. Simmons, J. Z. Salvail, P. Dluhy, H. Riemann, N. V. Abrosimov, P. Becker, H.-J. Pohl, J. J. L. Morton, and M. L. W. Thewalt, Science **342**, 830 (2013).
[30] M. Zhong, M. P. Hedges, R. L. Ahlefeldt, J. G. Bartholomew, S. E. Beavan, S. M. Wittig, J. J. Longdell, and M. J. Sellars, Nature (London) **517**, 177 (2015).
[31] R. Auccaise, J. Teles, R. Sarthour, T. Bonagamba, I. Oliveira, and E. deAzevedo, J. Magn. Reson. **192**, 17 (2008).
[32] V. K. Michaelis, E. Markhasin, E. Daviso, J. Herzfeld, and R. G. Griffin, Phys. Chem. Lett. **3**, 2030 (2012).
[33] F. A. Perras, T. Kobayashi, and M. Pruski, J. Am. Chem. Soc. **137**, 8336 (2015).